

Effect of Annealing on Sb_2S_3 Thin Film Deposited By Chemical Method

S. D. Lakade

*Bhausahab Nene College, Pen, (M.S.) India.
lakadesd@rediffmail.com*

Abstract— In the present paper, we have reported the room temperature growth of antimony sulphide (Sb_2S_3) thin films by dip method and detailed characterization of these films. The films were deposited from a reaction bath containing antimony chloride, glycine and sodium thiosulphate. We have analyzed the structure, morphology, composition properties of annealed Sb_2S_3 thin films. X-ray diffraction pattern showed that the films were polycrystalline. Scanning microscopy (SEM) study shows, size of the sphere gets increased as the annealing temperature increases. The globular grains are merged with one another. Composition analyses by EDAX show that the films are nearly stoichiometric in composition.

Keywords: *Thin films; X-ray diffraction; EDAX, Surface morphology.*

I INTRODUCTION

The semiconducting compounds are of great importance in electronic science in view of their photoconductivity, photoresistivity and thermoelectric power [1-2].

As an important V-VI group binary chalcogenide, antimony trisulfide with an energy band gap varying between 1.5 and 2.2 eV has attracted particular attention, owing to its good photovoltaic properties, high thermoelectric power, broad spectrum response, and suitable valence band position [3-5]. Some physical properties like photoelectric properties and the conduction and charge carrier transport mechanism have been reported in literature. [6-8]. It has special properties such as high refractive index, well defined quantum size effects [9-11] It is a n-type semiconductor [12]. This material has been applied in various areas such as television cameras with photoconducting targets, thermoelectric cooling devices, electronic and optoelectronic devices, solar energy conversion, visible light-responsive photocatalysis, microwave, switching devices, photovoltaic structures, resonant laser cavity and optical data storage devices [13-26]. It has been demonstrated that the properties of antimony trisulfide are determined predominantly by their crystal structure, size, and morphology. Therefore, the

synthesis of Sb_2S_3 materials with well-controlled size and shape is of great significance for their applications. Up to date, a variety of 1D nanostructures of Sb_2S_3 such as nanorods [27-30], nanowires [31], nanotubes [32-33], and nanoribbons [34] have already been synthesized by various methods. Several investigators have prepared Sb_2S_3 thin films with different chemical methods such as spray pyrolysis [35-36], chemical bath deposition [37-38], successive ionic layer adsorption and reaction method [39], electrodeposition [40], dip and dry method [41] and vacuum evaporation [42-43]. The dip method for formation of thin films from aqueous solution is a promising technique because of its simplicity and economics. The starting chemicals are universally available and inexpensive. This method can be used to deposit films at low temperature which avoids oxidation of the deposited material. The deposition conditions are easily controlled to get improved orientation and grain structure of the film. The dip method has the major advantage with respect to other methods is that the films on different kinds of substrate shapes, and sizes can be deposited. Considering the technical importance of this material, fabrication of Sb_2S_3 with some inspired structures such as a flower-like structure by a convenient and efficient method has always been a great interest. We report synthesis of Sb_2S_3 thin film by dip method. The deposited film samples were characterized by various techniques such as X-ray diffraction, scanning electron micrograph, EDAX, properties are also studied.

II EXPERIMENTAL DETAILS

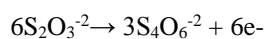
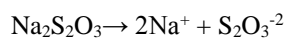
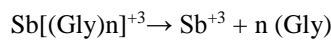
The substrates used for depositing the films were non-conducting glass slides of the size 75 x 25 x 2 mm. All the chemicals used for the deposition were of AR grade. All the solutions were prepared in double distilled water. The chemicals used were antimony chloride, glycine, and sodium thiosulphate. To prepare the bath, 10mL (0.2M) SbCl_3 was poured in 100mL beaker; other chemicals were used in the following sequence: 4mL (1M) glycine, 15mL (0.2M) sodium thiosulphate. The pH of the reactive mixture is 4.53. The total volume was made 50mL with double distilled water. The temperature of the bath was maintained at 278 K using ice bath. The solution was

stirred vigorously before dipping non-conducting glass substrates. The substrates kept vertically slightly tilted in a reactive bath. The temperature of the bath was then allowed to increase up to 298 K very slowly. The film was deposited on both sides of slides. After 5 hours, the slides were removed washed several times with double distilled water. The film was dried naturally and preserved in dark desiccators over anhydrous CaCl₂

III RESULT AND DISCUSSION

3.1 Growth Mechanism

The deposition process of Sb₂S₃ is also depends on the liberation of antimony and sulphide ions in the reaction bath. The free ions then combine ion via ion process on the glass or stainless steel substrates. Preparation of Sb₂S₃ film sample take place as the ionic product of antimony and sulphide ions larger compare to the solubility product of Sb₂S₃. [K_{sp}=1.5 x10⁻⁹³]⁴⁴The amount of antimony and sulphide free ions in the reaction bath determine the speed of Sb₂S₃ deposition. The amount of free antimony ions is maintained using glycine, that develops an ionic species Sb[(Gly)n]⁺³ using antimony ions. The chemical reactions occur for the deposition of Sb₂S₃ films may be express as given below;



In acidic conditions S₂O₃⁻³ may be disintegrates as follows

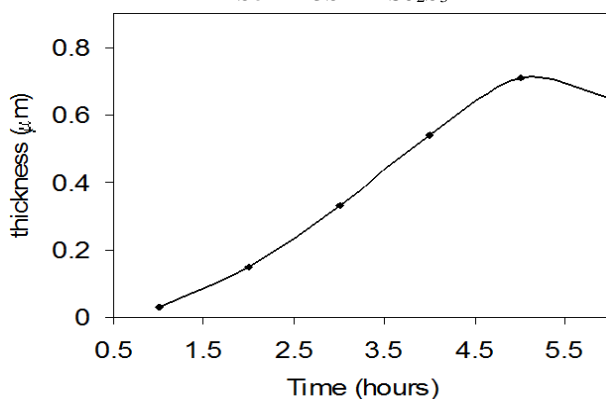
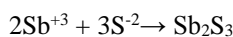
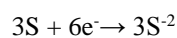
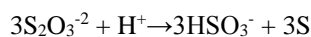


Figure 1: Plot of thickness against deposited time.

Deposition begins only when the chalcogenide concentration is high enough to allow nucleation to start, which occurs in the linear region of growth. As the limiting reactant is used up, growth will start slow down and eventually stop due to depletion of the reactant [45-46].

The film thickness was measured by weight difference method by using relation

$$t = m/\rho A \text{ ----- (1)}$$

Where, m is the mass of the film deposited on the substrate, A is the area of the deposited films and ρ is the density of deposited material (Sb₂S₃ = 4.64 g/cm³). The terminal thickness was found to be 0.71 μm. The behaviour of thickness versus deposition time is show in Fig.1. The film thickness increases with immersion time, but after 5 h the growth process reaches the saturation and further only lower thickness value can be achieved. This is mainly due to decrease in concentration of reactant with time as well as dissolution of the film in the solution. The deposited films are orange and transparent.

3.2 Structural Characterization

The X-ray diffractogram of annealed Sb₂S₃ thin samples synthesized on non-conducting templates such as glass are indicated in Figure 2 The polycrystalline nature of the samples is decided from numerous peaks in diffraction pattern. The examination of spectrum shows that the annealed samples have been belonging to orthorhombic phase for the entire temperature range under consideration. The diffused background is due to non crystalline templates as well as some amorphous nature present in Sb₂S₃ samples. The utmost strong reflection indicates that for Sb₂S₃ thin samples were begin from (101) peak.

Annealing of thin film at 348K enhance the intensity of the all plane. As a result there is increase in crystallinity of the sample. However, (351) peak disappear from the Sb₂S₃ pattern. Films annealing at 423 K initiate additional peaks at d = 1.701 Å (132). Annealing at 473K provide new peaks at d = 1.554 Å (242). The peak intensity increases with rise in temperature suggesting increasing crystallinity of samples. As the annealing temperature rise, the peak position slightly shifted towards the left side of the diffractogram. All thin films indicate the majority preferred plane (101) as well as other (310) and (230)

(211) (221) (510) (431) (132) (242) prominent reflections. No other peak in addition these are found out that suggests the annealed sample remains in single phase orthorhombic structure. The slight increase in the d magnitude of important peaks suggests that because of annealing, the material is very slightly expanding. Thus the cell symmetry is not varied by annealing.

Alter in lattice parameters has too been found out for the entire samples. The lattice factors have been estimated by applying equation

$$(1/d^2) = (h^2/a^2 + k^2/b^2 + l^2/c^2) \text{-----(2)}$$

It is found out that as annealing temperature of the sample go up, the lattice factor 'a' differ gradually from 11.260 (Annealing temperature = 348 K) to 11.367 Å (Annealing temperature = 473 K). The lattice factor 'b and c' enhance correspondingly from 11.331 to 11.509 Å and 3.852 to 3.898 Å as the annealing temperature raise. The expansion of the cell is decided by measuring the volume of the lattice. The volume is estimated with the help of equation

$$V = abc \text{----- (3)}$$

for the entire the sample. As the annealing temperature go up the volume too raise. For temperature 348 K having lowest volume whilst temperature 478 K having highest volume. The value of volume varies from 491.46 to 509.94 (Å)³.

The average particle dimensions become determined by using Scherrer's method

$$D = 0.9\lambda / \beta \cos\theta \text{----- (4)}$$

The average particle dimension is estimated via taking into account the maximum intensity peak. The average particle size for the all samples remains in the range of 156.33 to 169.26 nm.. The microstrain produce in the entire samples have been estimated using equation

$$\epsilon = \beta \cos\theta / 4 \text{----- (5)}$$

It is observed that the microstrain reduce with enhance in annealing temperature. The magnitude of microstrain is 2.217 x 10⁻³ for annealing temperature at 348 K and 2.132 x

10⁻³ for sample annealed at 478 K. This is because of the predominant recrystallization technique in the polycrystalline thin samples and because of the movement of interstitial antimony atoms from within the particles to its grain boundary that dissolve and result in a decrease in the lattice defect.

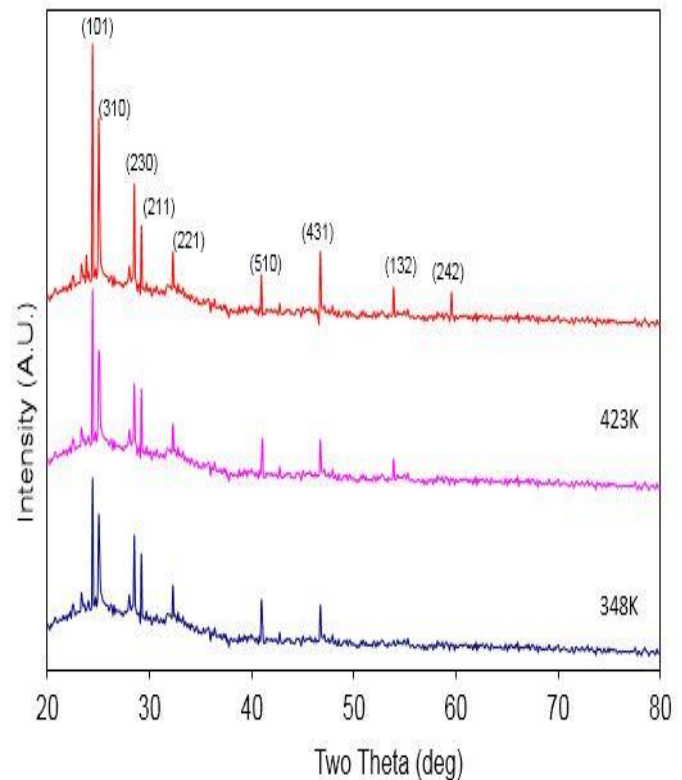


Figure 2 -X-ray diffraction pattern of annealed Sb₂S₃ sample.

Dislocation density is determined using the expression

$$\delta = n/D^2 \text{----- (6)}$$

The magnitude of dislocation density became observed to be 4.091 x 10¹⁵m⁻² for annealing temperature 348 K and 3.49 x 10¹⁵ m⁻² for sample annealed at 478 K. The dislocation density decreased as the annealing temperature and crystallite dimension enhance.

3.3 Morphological and Compositional Study

The scanning electron micrograph of annealed Sb₂S₃ sample at different temperature is represented in Figure. 3(a-c). Sphere-shaped and bunches of fiber resembling arrangement became observed. The size of the sphere gets increased as the annealing temperature increases. The globular grains are merged with one another. The threads are randomly distributed.

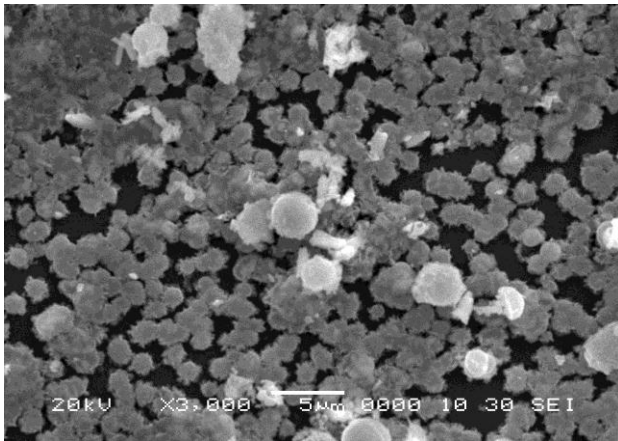


Figure 3 (a) Scanning electron image of annealed Sb_2S_3 sample at 348K.

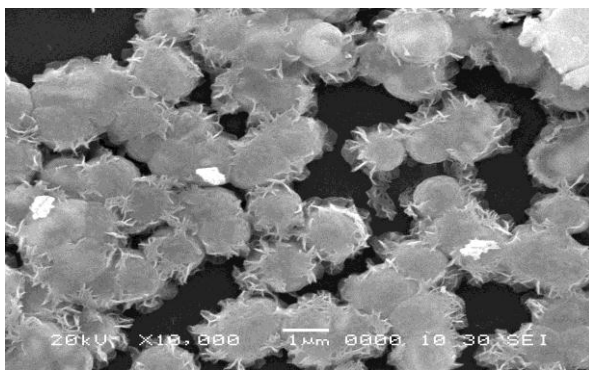


Figure 3 (b): Scanning electron image of annealed Sb_2S_3 sample at 423K.

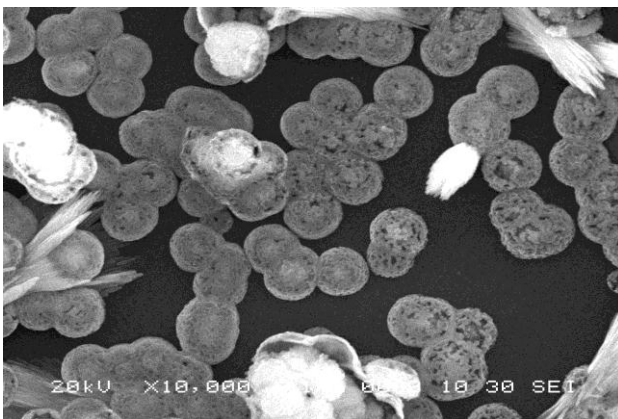


Figure 3 (c): Scanning electron image of annealed Sb_2S_3 sample at 473K.

Figure 4 shows a typical EDAX pattern of Sb_2S_3 thin films. The elemental analysis was carried out only for Sb and S; the average atomic percentage of Sb: S was 46.22: 53.78, showing that the film is slightly rich in S^{-2} and well agree well with the result reported by Mane et al [47]

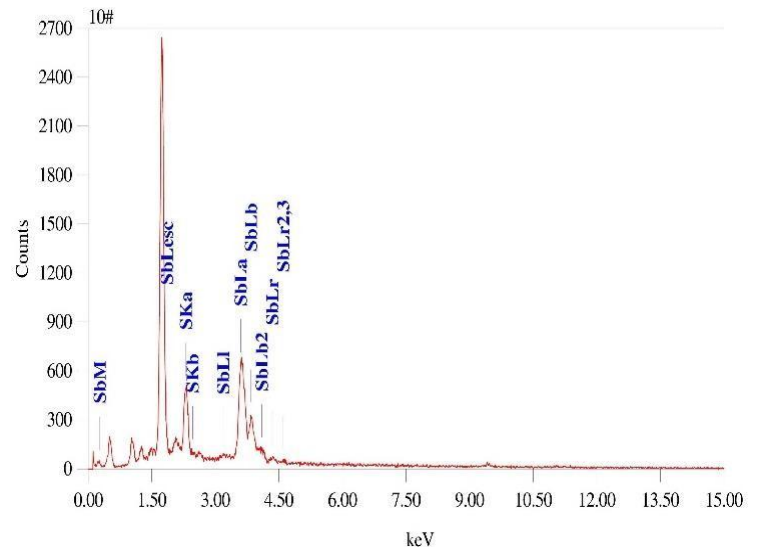


Figure 4: EDAX of Sb_2S_3 thin films

IV CONCLUSION

- 1) Sb_2S_3 can be deposited at room temperature by chemical method.
- 2) The film formation takes place via nucleation and growth.
- 3) Films were orange, polycrystalline in orthorhombic structure.
- 4) The size of the sphere gets increased as the annealing temperature increases. The globular grains are merged with one another.

REFERENCES

- [1] S.R. Gadakh, C.H.Bhosale, Mater. Chem. Phys.78 (2002) 367.
- [2] G. Ghosh, B.P.Verma, Thin Solid Films 60 (1979) 61.
- [3] X. Shuai, W. Shen, Nanoscale Res. Lett. 7 (2012) 199.
- [4] S. Ibuke, S. Yochimatsu, J. Phys. Soc. Jpn 10 (1955) 549,
- [5] K. Li, F. Huang, X. Lin, Scripta Mater. 58 (2008) 834.
- [6] Mary. J. Chockalingam, K. Nagaraja Rao, N. Rangarajan, C.V. Suryanarayana, J. Phys. D: Appl. Phys. 3 (1970) 1641.
- [7] E. Montrimas, A. Pazera, Thin Solid Films 34 (1976) 65.
- [8] N. Mathew, R.Oommen, U. Rajalakshmi, Chalcogen. Lett. 7 (2010) 701.
- [9] C. Lokhande, B. Sankapal, R. Mane, H. Pathan, M. Muller, M. Giersig, V. Ganesan, Appl. Surf. Sci. 193 (2002) 1.
- [10] A.Salem, M. Selim, J. Phys. D Appl. Phys. 34 (2001) 12
- [11] B. Krishnan, A. Arato, E. Cardenas, T. Roy, G. Castillo Appl. Surf. Sci. 254, (2008) 3200.
- [12] K.Y. Rajpure, C.H. Bhosale, Mater. Chem. Phys. 64 (2000) 14.
- [13] D. Arivuoli, F. Gnanam, P. Ramasamy, J Mater Sci. Lett 7 (1988) 711.
- [14] O. Savadogo, K. Mandal, SolEner. Mater Sol. Cells 26 (1992) 117.
- [15] Q. Han, L. Chen, M. Wang, X. Yang, L. Lu, X. Wang, Mater Sci Eng. B 166 (2010) 118.

- [16] M. Sun, D. Li, W. Li, Y. Chen, Z. Chen, Y. He, X. Fu, J. Phys Chem C 112, (2008) 18076.
- [17] X. Cao, L. Gu, L. Zhuge, W. Gao, W. Wang, S. Wu, Adv. Funct. Mater. 16, (2006) 896.
- [18] I. Zawawi, A. Moez, F. Terra, M. Mounir, Thin Solid Films 324(1998) 300.
- [19] N. Mathew, R. Oommen, U. Rajalakshmi, C. Sanjeeviraja, Chalcogen. Lett. 8, (2011) 441.
- [20] S. Messina, M. Nair, P. Nair, Thin Solid Films. 515 (2007) 5777.
- [21] Y. Lazcano, M. Nair, P. Nair, J. Electrochem. Soc 152 (2005) 635.
- [22] R.S. Mane, C.D. Lokhande, Mater. Chem. Phys. 78 (2003) 385.
- [23] O. Savadogo, Sol. Ener. Mater. Sol. Cells. 52 (1998) 361.
- [24] E. Perales, G. Lifante, F. Rueda, C. Hares, J. Phys. D: Appl. Phys. 40 (2007), 2440.
- [25] E. Perales, F. Rueda, J. Lamela, C. Heras, J. Phys. D: Appl. Phys. 41 (2008), 45403.
- [26] P. Arun, A. Vedeshwar, N. Mehra, Mater. Res. Bull. 32 (1997) 907.
- [27] J. Ota, S. Srivastava, J. Cryst Growth 7 (2007) 343.
- [28] P. Estevané, M. Sánchez, Mater Lett 64 (2010) 2627.
- [29] J. Ota, P. Roy, S. Srivastava, B. Nayak, A. Saxena, J. Cryst Growth 8 (2008) 2019.
- [30] A. Alemi, S. Joo, Y. Hanifehpour, A. Khandar, A. Morsali, B. Min J Nanomater 10 (2011) 528.
- [31] Z. Geng, M. Wang, G. Yue, P. Yan. J Cryst Growth 310 (2008) 341
- [32] J. Yang, Y. Liu Y, H. Lin, C. Chen, Adv Mater. 16 (2004) 713.
- [33] X. Cao, L. Gu, W. Wang, W. Gao, J. Zhuge, Y. Li J Cryst Growth 286 (2006) 96.
- [34] Y. Yu, R. Wang, Q. Chen, L. Peng, J PhysChem B 110 (2006) 13415
- [35] C. Bhosale, M. Uplane, P. Patil, C. Lokhande, Thin Solid Films 248(1994) 137.
- [36] V. Killedar, C. Lokhande, C. Bhosale, Mater. Chem. Phys. 47 (1997) 104
- [37] R. Mane, B. Sankpal, C. Lokhande, Thin Solid Films 353 (1999) 29.
- [38] J. Desai, C.D. Lokhande, Thin Solid Films 237 (1994) 29.
- [39] B. Sankpal, H. Pathan, C. Lokhande, J. Mater. Sci. Lett. 18 (1999) 1453.
- [40] N. Yesugade, C. Lokhande, C. Bhosale, Thin Solid Films 263 (1995) 145.
- [41] B. Nayak, H. Acharya, T. Choudhuri, G. Mitra, Thin Solid Films 92 (1982) 309.
- [42] N. Tigau, C. Gheorgies, G. Rusu, S. Bota, J. Non-Cryst. Solids 351(2005) 987.
- [43] N. Tigau, Cryst. Res. Technol. 42 (2007) 281
- [44] R. Weast, CRC Handbook of Chem. Phys. 69 edition. Boca Raton: CRC Press; 1988.
- [45] G. Godes, Chemical Solutions Deposition of Semiconductor Films, Marcel Dekker, 2003.
- [46] H.E. Esparza-Ponce, J. Hernandez-Borja, A. Reyes-Rojas, M. Cervantes-Sanchez, Y.V. Vorobiev, R. Ramirez-Bon, J.F. Perez-Robles, J. Gonzalez-Hernandez, Mater. Chem. Phys. 113 (2009) 824.
- [47] R.S. Mane, C.D. Lokhande, Surf. Coat. Technol. 172 (2003) 51.